PHYSICAL REVIEW E **70**, 020401(R) (2004)

Grain boundary dynamics under mechanical annealing in two-dimensional colloids

Q. H. Wei* and X. L. Wu†
Department of Physics and Astronomy, University of Pittsburgh, Pittsburgh, Pennsylvania 15260, USA
(Received 4 April 2003; published 31 August 2004)

Two-dimensional (2D) colloids embedded in a soap film are employed to study the structures and dynamics of grain boundaries (GBs). While a soap film is drawn vertically from a concentrated bulk suspension, the colloidal particles self-assemble to form polycrystalline structures with a typical grain size of about 100 lattice spaces. Studies of these grain boundaries reveal that the GB lines are faceted at "atomic" scale, leading to a constant energy per unit length along each line. The measured GB energy as a function of misfit angle is in agreement with Reed-Shockley's theoretical predictions. When an external mechanical vibration is applied to the bulk suspension, the grain boundaries are observed to migrate and grains to rotate under the stress field induced by the vibration. The total length of the grain boundaries is found to diminish logarithmically with time, with the rate constant being a function of the excitation strength. This phenomenon, called "mechanical annealing," provides a robust means to grow large 2D single-domain crystals.

DOI: 10.1103/PhysRevE.70.020401 PACS number(s): 82.70.Dd, 61.72.Mm

Grain boundaries (GBs), which are the longest known crystal defects [1,2] play a critical role in the properties of many materials such as ceramics, metals, and semiconductors [3]. The energy needed to create a GB is a function of its orientation with respect to a crystallographic axis characterized by the angle φ and the misfit angle θ of the two neighboring grains as shown in Fig. 1(c). While many static structures of GBs are known due to x-ray diffraction and electron microscopy techniques [3,4], the dynamics of GB motion driven by thermal fluctuations or an external stress field, i.e., the texture evolution, is much harder to study. As a result, the physical mechanisms remain largely unknown [5–8]. We utilize a colloidal system for the first time to study GB structures and dynamics in a freely suspended soap film.

Studies of these GB structures, which form near equilibrium, reveal that they are faceted at "atomic" scales with $\varphi=0$, implying that the energy is constant along the GB. By measuring the occurring probability of grain boundaries as a function of their misfit angle θ we obtained GB energy $E(\theta)$, which is shown to be in good agreement with the Read-Shockley prediction in a two-dimensional (2D) system. An interesting observation is that external periodic vibrations of $\sim$100 Hz can induce GB migration and grain rotation when the vibration energy E_V is sufficiently large. Under certain conditions, all GBs can be eliminated, resulting in a large single-domain crystal. Furthermore, the total length of GBs is found to decay logarithmically in time with a decay rate increasing with E_V.

Our experimental setup is similar to the one used previously with minor changes [9]. A schematic diagram of the setup is shown in Fig. 1(a). The particles used are monodispersed 1μm diameter polystyrene beads, which behave like hard spheres. The 2D film of colloidal monolayer is formed by dipping a thin plastic frame into the bulk suspension, containing $\sim$33% solid volume of particles, and withdrawing it slowly upwards. Owing to gravity, the film thins to a thickness comparable to the particle size, leading to the curving of the water/air interfaces between particles. This curved meniscus exerts an attractive capillary force between particles, causing them to self-assemble into a 2D array [9]. Simple calculations show that the capillary force is much stronger than the electrostatic force and thus dominates the particle-particle interaction [10]. The kinetics of self-assembly are rapid and robust in that once the 2D array is

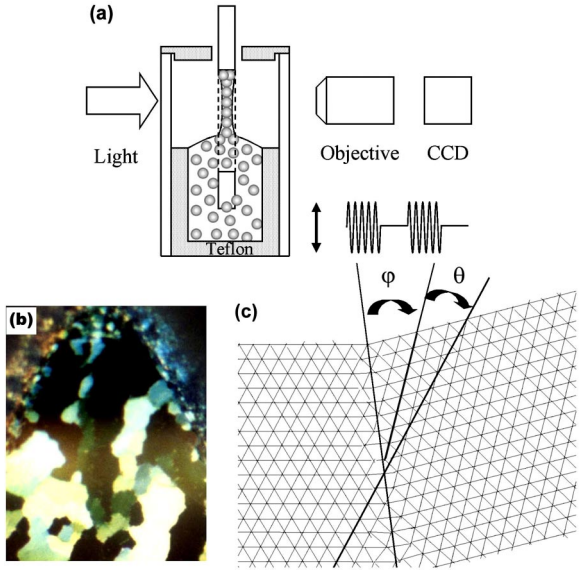

FIG. 1. (Color online) (a) Experimental setup. The top sketch provides a side view from a direction parallel to the plastic frame. The inner cell is made of Teflon. The thin plastic frame has a rectangular hole that supports the 2D colloidal crystal film. The Teflon cell is kept in a larger glass cell that is covered on the top by a Teflon cap to keep the humidity inside the cell constant. (b) The dark-field microscopic picture of a typical polycrystalline colloidal film. (c) A sketch for the definition of grain boundary misfit angle θ and the grain boundary orientation angle φ.

*Electronic address: Qihuo.Wei@osa.org
†Electronic address: xlwu@pitt.edu

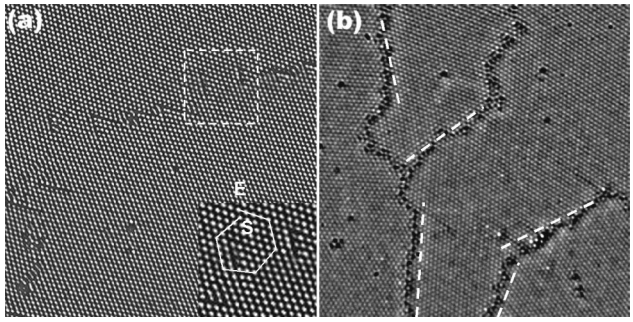

FIG. 2. Microscopic morphology of GBs. (a) Typical structures of small-angle GBs consists of separated wedge- (<) or line-shaped (—) defects. The inset shows that < shaped defects are actually dislocations. The white line is the Burgers circuit with the Burgers vector connecting points S and E. (b) Typical configurations of large-angle GBs. The white dashed lines show that the GBs are parallel to the crystalline graphic axes.

formed, it can last almost indefinitely in a high humidity environment. This "frozen-in" structure is metastable, reflecting a particular particle conformation at the moment of film formation when the ambient temperature is 25 °C.

We illuminate the colloidal array with a white-light source from behind the film and image the crystal structures using a video camera equipped with a 20× (or 50×) long-working-distance optical microscope objective. The GBs appear either as black lines between homogeneous bright domains of crystal grains (normal transmission microscopy) when light impinges perpendicularly to the film, or as the border lines between mosaics of colored domains [Fig. 1(b), color for online version] due to Bragg diffractions (dark-field microscopy) when the light shines on the film with an incident angle of ~60°. We noted that owing to the absence of multiple scattering, the color from Bragg diffraction in the 2D crystal is much more vivid than that seen in three-dimensional (3D) colloidal crystals.

Mechanical vibrations at an acoustic frequency are applied to the bulk suspension by mounting the sample cell on a loudspeaker that is excited vertically by a sinusoidal wave from a signal generator. The acoustic wave can efficiently transmit kinetic energy to the particles, causing them to move in the film. To make sharp images of the particles, we excite the film with pulse trains of sinusoidal waves each lasting about 0.5 s with a 1.5 s interval between adjacent pulses. The frequency of the sinusoidal signals is 120 Hz, corresponding to 60 oscillations within a single pulse. Snapshots are taken during the quiescent period between the vibrations. A sequence of pictures taken at different times shows the evolution of the microdomain structures of colloids in the film.

In the following, we report measurements without vibrations. The 2D crystals obtained in this case are polycrystalline [Fig. 1(b), color for online version], where the color mosaic domains correspond to different Bragg diffracted colors or different crystal orientations. Using the 50× magnification objective, the small- and large-angle GBs can be easily identified, which are shown in Figs. 2(a) and 2(b), respectively. It can be seen that small-angle GBs are composed of sequences of wedge- (<) or line-shaped (−) defects

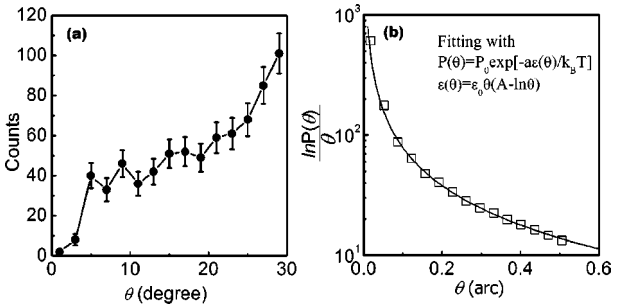

FIG. 3. (a) The measured probability of the misfit angle θ. The error bars are standard deviations. (b) $P(\theta)$ is the normalized probability of θ. The solid curve is the fit to the theoretical curve $P(\theta)=P_0\exp[-aE(\theta)/k_BT]$.

that are actually dislocations. If one tries to construct a hexagon loop surrounding the inner core as in the inset of Fig. 2(a), this so-called Burgers circuit fails to close itself, indicating a dislocation characterized by the Burgers vector. Despite the fact that the cores of dislocations appear to be quite normal, i.e., the nearest neighbors of each particles are composed of seven- and fivefold disclinations [11], certain GB structures seen in our system are different from other colloidal and magnetic bubble systems [12,13]. For instance, the wedge- and line-shaped defects have not been reported in those systems. This difference in the GB structure may be attributed to the different particle interactions in the 2D film or the buckling of particles into the third dimension, perpendicular to the film.

The large-angle GBs of our system also possess interesting features. Though they are irregular on macroscopic scales [black lines in Figs. 4(a)–4(f)], on microscopic and mesoscopic scales the lines are faceted. In other words, the interfaces are most likely to be along one of the six possible crystalline axes of the two grains. This is indicated by the white dashed lines in Fig. 2(b). Thus, the orientation of large-angle GBs assumes a nearly constant value $\varphi=0$, leading to θ being the only remaining degree of freedom of the large-angle GBs in our system. This seems to be the natural choice because the GB energy density remains constant along the boundary between two grains. This is, however, in contrast to 3D systems where GBs are commonly observed to lie in a symmetrical position between the neighboring grains [3,4]. Although faceted GBs have also been observed in three dimensions, their formation is found to be correlated with impurity contents, and thus attributed to residual impurities rather than energetic reasons [3,4].

In order to estimate the energy associated with the GBs, we measured the probability density function $P(\theta)$ of the misfit angle θ with no external vibration, where $P(\theta)d\theta$ is defined as the probability of a GB with a misfit angle between θ and $\theta+d\theta$. If the system is near equilibrium, $P(\theta)$ is just the nucleation probability of a GB, which can be related to the energy $E(\theta)$ by the Boltzmann distribution: $P(\theta)=P_0\exp[-aE(\theta)/k_BT]$. Here, k_BT is the thermal energy, P_0 is the normalization constant, and a is the lattice spacing of the 2D crystal. Because of the sixfold symmetry of the lattice and fixed φ, the maximum misfit angle can vary between 0° and 30°. The measured $P(\theta)$ is delineated in Fig. 3, which

represents an average over more than 700 independent adjoining GB pairs. It is evident from the figure that the large-angle GBs are statistically more favorable than the small-angle ones, implying that they take less energy to form. Another interesting feature of the probability function $P(\theta)$ is a sudden drop for $\theta < 5°$. Naively, one would expect that the energy associated with the GBs of a very small misfit angle is small, corresponding to a high probability of occurrence. This certainly is not what was observed in the measurement. This peculiar effect can be explained by the kinetics of GB formation, i.e., for the given noise level k_BT, GBs with energy per dislocation $aE(\theta) \leqslant k_BT$ are spontaneously annealed during crystal formation and are thus not observed in the measurement. During the experiments, the rapid disappearing of small-angle GBs by the dislocation movements was indeed observed.

Based on a linear elastic theory, Read and Shockley have given an analytic expression for the GB energy $E(\theta)$ per lattice spacing in terms of θ and φ [1]

$$\varepsilon(\theta) = aE(\theta) = \varepsilon_o\theta[A - \ln(\theta)], \tag{1}$$

where ε_0 and A are slow varying functions of φ and can be considered as constants. The theory assumes the crystal to be isotropic, characterized by two Lamé coefficients, which is indeed the case for a 2D triangular lattice. Physically, the $\varepsilon_0\theta A$ term in Eq. (1) represents the energy of individual dislocations, and the second term $\varepsilon_0\theta\ln(\theta)$ is due to the interactions between the dislocations. It is believed and also experimentally observed in some 3D systems [14] that this result is valid not only for small-angle GBs but also for large-angle ones, although its theoretical justification is questionable. In the current experiment, θ was measured up to 30° and the small-angle approximation will be assumed. In the limit $\varphi = 0$, the parameters in Eq. (1) are simplified with the result: $\varepsilon_0 = Ka^2/8\pi$ and $A = E_c - Ka^2\ln(2\pi)/8\pi$, where K is the Young's modulus, a is the particle spacing, and E_c is the dislocation core energy. A few of our observations are consistent with the Read-Shockley predictions [1,15]. One can plot $\ln P(\theta)/\theta$ as a function of $\ln\theta$. The slope of the plot, delineated in Fig. 3(b) yields $\varepsilon_0/k_BT = 11$, which gives the Young's modulus of 1.1×10^{-3} erg/cm^2 for these embedded 2D colloidal crystals. Comparing with the vibration energy needed to induce the GB migrations (to be discussed below), the energy scale of ε_0 is of the same order of magnitude of the vibration energy.

We next investigate the effect of external vibration on the coarsening of GBs. The vibration energy is coupled to the particles in the soap film because the bottom of the film is in contact with the bulk suspension. In order to characterize the vibration strength, we define an energy scale E_V, which is the average kinetic energy of a particle near the bulk liquid surface normalized by the thermal energy, $E_V = 4\pi^2mf^2Z^2/k_BT$. Here m is the particle mass, f is the vibration frequency, Z is the vibration amplitude, k_B is the Boltzmann constant, and T is the absolute temperature.

After the application of vibrations, the GBs are observed to migrate and to shrink in length. A series of pictures taken at different times in Fig. 4 show how GBs evolve with time.

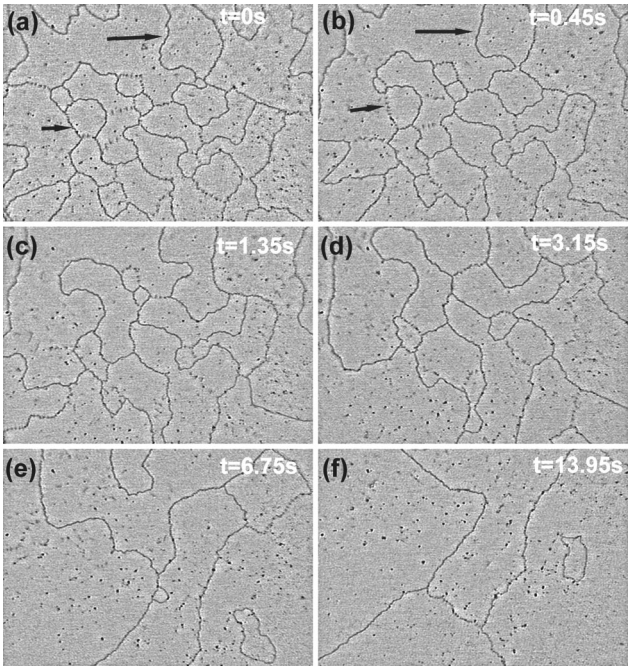

FIG. 4. Snapshots of GB evolution under vibration. The normalized vibration energy $E_V = 105$ is fixed, and the time t is indicated in each picture.

Typically one observes that GBs decrease in number and are finally eliminated. The detail of GB migration is, in general, rather complex because the mobility of a GB depends not only on the misfit angle θ, but also on the local stress field. As a result, the mobility is not a constant, but varies along the GB. However, simple features can be extracted: (1) A GB simply translates normally to its orientational direction, resulting in the shrinkage of one domain and the growth of the other. In the process, the GB is straightened, reducing the surface energy of the boundary as indicated by long arrows in Figs. 4(a) and 4(b). (2) A large-angle GB transforms to a small-angle one which disappears rapidly through the fast motion of dislocations, as indicated by short arrows in Figs. 4(a) and 4(b). It is obvious that such a transformation must be accompanied by a relative rotation of the two neighboring grains, implying that the net torque acting on the grains is not zero. These observations are in agreement with previous experimental and computer simulations for atomic systems in three dimensions [6–8].

In order to investigate the global evolution of the GBs with time, the total lengths of GBs are measured. The total length L, if multiplied by a unit GB energy averaged over different misfit angles θ, is a measure of the total GB energy. Shown in Fig. 5 is the measured L of GBs as a function of time for three different vibration amplitudes. Though the data are admittedly noisy for individual runs, the trend however is clear and is consistent with the logarithmic decay of the form $L \sim -\alpha\ln(t) + L_0$. We note that as the vibration energy E_V increases, the decay rate α on this logarithmic time scale also increases and approximately $\alpha \sim E_V^{1/3}$. For a sufficiently large vibration energy ($E_V = 105$), such as the last curve shown in Fig. 5, a steady state with $dL/dt = 0$ can be reached with L being a constant at long times.

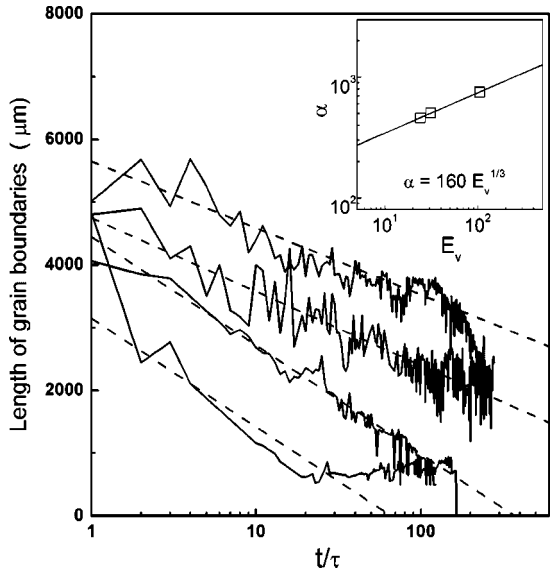

FIG. 5. The total length of GBs vs time for three different vibration energies: E_V=24, 31, 105, and 105 arranged from the top to the bottom. The last two runs (E_V=105) are duplicates but with different initial conditions. The dashed lines are fittings to $L\sim -\alpha\ln(t)+L_0$. The inset shows the fitted value α vs the vibration energy E_V (squares) where the solid line is the fitting $\alpha\sim E_V^{\beta}$ with $\beta\approx 0.33$.

This behavior is a result of the competition between annealing and creation of new GBs when the external force is significantly large. However, even under such a strong external excitation, the logarithmic decay is still observed in the intermediate times as demonstrated by the last two curves in Fig. 5.

In summary, we have utilized a 2D system of colloidal particles embedded in a soap film to study the physics associated with GBs. A way of measuring GB energy has been demonstrated by using the probability density function of the misfit angle θ. We also investigated the dynamics of GBs driven by external mechanical vibrations. It is shown that the GB evolves through curvature reduction and grain rotation, and that the total length of grain boundaries decays logarithmically with time. The observation of the logarithmic decay is new and intriguing because most theoretical models based on curvature-driven [16] or rotation-induced [8,17] grain growth predict power-law behavior in long times. However, the logarithmic growth was predicted in a more sophisticated model in which the GB curvature is coupled to the rotational degrees of freedom [18,19]. The coarsening dynamics seen in our system also bear resemblance to glasses where frustrations conspire to create energy barriers on different scales, resulting in dynamics that are "sluggish" and decay in a logarithmic fashion [20–22]. As shown recently by Boyer and Viñals, such slow dynamics can indeed be solutions of the Swift-Hohenberg model of pattern formation even in the absence of quenched disorder [21,22]. The problem of GB dynamics is a significant one and is largely unsolved. This calls for more concerted efforts between theory and experiments.

The authors would like to thank Mike Rivera for helpful discussions. The financial supports from NASA and NSF are acknowledged.

[1] W. T. Read, Jr., *Dislocations in Crystals* (McGraw-Hill, New York, 1953).
[2] W. T. Read and W. Shockley, Phys. Rev. **78**, 275 (1950).
[3] B. Chalmers, J. W. Chritian, and T. B. Massalski, *Progress in Material Science* (Pergamon, New York, 1972), Vol. 16.
[4] G. A. Chadwick and D. A. Smith, *Grain Boundary Structure and Properties* (Academic, New York, 1976).
[5] G. Gottstein and L. S. Shvindlerman, *Grain Boundary Migration in Metals* (CRC, London, 1999).
[6] L. Margulies, G. Winther, and H. F. Poulsen, Science **291**, 2393 (2001).
[7] K. L. Merkle, L. J. Thompson, and F. Phillipp, Phys. Rev. Lett. **88**, 225501 (2002).
[8] D. Moldovan, V. Yamakov, D. Wolf, and S. R. Phillpot, Phys. Rev. Lett. **89**, 206101 (2002).
[9] Q. H. Wei, D. M. Cupid, and X. L. Wu, Appl. Phys. Lett. **77**, 1641 (2000).
[10] P. A. Kralchevsky and K. Nagayama, Langmuir **10**, 23 (1994).
[11] D. R. Nelson and B. I. Halperin, Phys. Rev. B **19**, 2457 (1979).
[12] C. A. Murray and D. H. Van Winkle, Phys. Rev. Lett. **58**, 1200 (1987).
[13] R. Seshadri and R. M. Westervelt, Phys. Rev. Lett. **66**, 2774 (1991).
[14] C. G. Dunn, F. W. Daniels, and M. J. Bolton, J. Met. **2**, 1245 (1950); K. T. Aust and B. Chalmers, Proc. R. Soc. London, Ser. A **204**, 359 (1951); N. A. Gjosten and F. N. Rhines, Acta Metall. **7**, 319 (1959).
[15] D. S. Fisher, B. I. Halperin, and R. Morf, Phys. Rev. B **20**, 4692 (1979).
[16] J. E. Burke and D. T. Yurnbull, Prog. Met. Phys. **3**, 220 (1952).
[17] D. Moldovan, D. Wolf, S. R. Phillpot, and A. J. Haslam, Philos. Mag. A **82**, 1271 (2002).
[18] A. E. Lobkovsky and J. A. Warren, J. Cryst. Growth **225**, 282 (2001).
[19] J. A. Warren, R. Kobayashi, A. E. Lobkovsky, and W. C. Carter, Acta Mater. **51**, 6035 (2003).
[20] J. A. Mydosh, *Spin Glasses: An Experimental Introduction* (Taylor & Francis, London, 1993).
[21] D. Boyer and J. Viñals, Phys. Rev. E **63**, 061704 (2001).
[22] D. Boyer and J. Viñals, Phys. Rev. E **65**, 046119 (2002).